Lattice calculation of the π^0, η and η' transition form factors and the hadronic light-by-light contribution to the muon $g-2$

arxiv:2305.04570

Antoine Gérardin
Willem Verplanke*
Gen Wang
[On Behalf of the Budapest-Marseille-Wuppertal Collaboration]

August 1st, 2023 40th International Symposium on Lattice Field Theory (LATTICE23), Fermilab

Centre de Physique Théorique

A*Midex Initiative d'excellence Aix-Marseille

anr agence nationale de la recherche

Motivation

- The error on the theory calculation of the muon $g-2$ is dominated by two hadronic contributions.

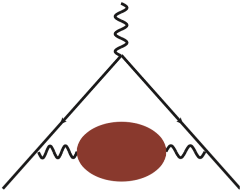

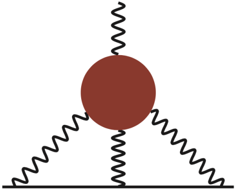

	LO HVP	**HLbL**
Contribution to $a_\mu \times 10^{11}$:	6931 ± 40	90 ± 17 [WP, 2020]

- An error of $\sim 10\%$ on the HLbL is needed for future experimental precision.
  → Difficult because it's a four-point function.
- Two independent approaches to calculate the HLbL contribution
  1. Direct lattice calculation of the four-point function.
  2. Dispersive: data-driven (cross-section, form factors).

  → Lattice QCD can provide valuable input to dispersive approach.
  → Agreement between two approaches is an important cross-check!

Motivation

https://muon-gm2-theory.illinois.edu/white-paper/

Contributions	Value $\times 10^{11}$
π^0, η, η'-poles	93.8(4.0)
π, K-loops/boxes	-16.4(0.2)
$\pi\pi$ scattering	-8(1)
scalars + tensors	-1(3)
axial vectors	6(6)
u, d, s-loops / short distance	15(10)
c-loop	3(1)
Total	92(19)

1. π^0-pole
    - Contribution has been determined on the lattice by Mainz (Gérardin et al., 2016, 2019). Preliminary results by ETM (Burri et al., 2022) (+ talk by Burri 01/08).
    - Also computed in data-driven dispersive framework (Hoferichter et al., 2018).
2. η, η'-pole
    - No dispersive results. Transition form factor not well-known in relevant kinematical region (experimentally).
    - But $\sim 1/3$ of the total pseudoscalar pole contribution
    - Challenges for lattice QCD: mixing between η, η' and sizable disconnected diagrams.

Motivation

https://muon-gm2-theory.illinois.edu/white-paper/

Contributions	Value $\times 10^{11}$
π^0, η, η'-poles	93.8(4.0)
π, K-loops/boxes	-16.4(0.2)
$\pi\pi$ scattering	-8(1)
scalars + tensors	-1(3)
axial vectors	6(6)
u, d, s-loops / short distance	15(10)
c-loop	3(1)
Total	92(19)

This work: the first lattice QCD calculation of the π^0-, η- and η'-pole contributions to the muon $g-2$ at the physical point and in the continuum limit.

Motivation

- In the dispersive framework, the 'master equation' relates the Pseudoscalar Transition Form Factors (**TFFs**) to pseudoscalar (p) pole contributions to a_μ^{p-pole} (Knecht and Nyffeler, 2002)

$$a_\mu^{p-pole} = \left(\frac{\alpha_e}{\pi}\right)^3 \int_0^\infty dQ_1 \int_0^\infty dQ_2 \int_{-1}^{1} d\tau \left[w_1(Q_1,Q_2,\tau)\mathscr{F}_{p\gamma^*\gamma^*}(-Q_1^2,-Q_3^2)\mathscr{F}_{p\gamma^*\gamma^*}(-Q_2^2,0) \right.$$
$$\left. + w_2(Q_1,Q_2,\tau)\mathscr{F}_{p\gamma^*\gamma^*}(-Q_1^2,-Q_2^2)\mathscr{F}_{p\gamma^*\gamma^*}(-Q_3^2,0) \right]$$

- $Q_3^2 = Q_1^2 + Q_2^2 + 2\tau Q_1 Q_2$
- $\tau = \cos\theta$
- θ angle between Q_1 & Q_2

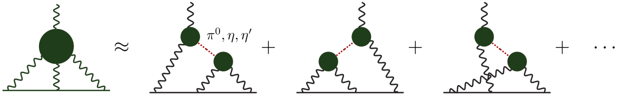

Motivation

- In the dispersive framework, the 'master equation' relates the Pseudoscalar Transition Form Factors (**TFFs**) to pseudoscalar (p) pole contributions to a_μ^{p-pole} (Knecht and Nyffeler, 2002)

$$a_\mu^{p-pole} = \left(\frac{\alpha_e}{\pi}\right)^3 \int_0^\infty dQ_1 \int_0^\infty dQ_2 \int_{-1}^{1} d\tau \, \Big[w_1(Q_1, Q_2, \tau) \mathscr{F}_{p\gamma^*\gamma^*}(-Q_1^2, -Q_3^2) \mathscr{F}_{p\gamma^*\gamma^*}(-Q_2^2, 0) + w_2(Q_1, Q_2, \tau) \mathscr{F}_{p\gamma^*\gamma^*}(-Q_1^2, -Q_2^2) \mathscr{F}_{p\gamma^*\gamma^*}(-Q_3^2, 0) \Big]$$

We recognize two main objects

1. The TFFs $\mathscr{F}_{p\gamma^*\gamma^*}(q_1^2, q_2^2)$
2. The weight functions $w_i(q_1, q_2, \tau)$

$\mathscr{F}_{p\gamma^*\gamma^*}(q_1^2, q_2^2)$ encodes the interaction between a pseudoscalar and two virtual photons.

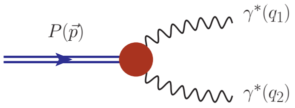

Motivation

- In the dispersive framework, the 'master equation' relates the Pseudoscalar Transition Form Factors (**TFFs**) to pseudoscalar (p) pole contributions to a_μ^{p-pole} (Knecht and Nyffeler, 2002)

$$a_\mu^{p-pole} = \left(\frac{\alpha_e}{\pi}\right)^3 \int_0^\infty dQ_1 \int_0^\infty dQ_2 \int_{-1}^{1} d\tau \, \Big[w_1(Q_1, Q_2, \tau) \mathcal{F}_{p\gamma^*\gamma^*}(-Q_1^2, -Q_3^2) \mathcal{F}_{p\gamma^*\gamma^*}(-Q_2^2, 0) + w_2(Q_1, Q_2, \tau) \mathcal{F}_{p\gamma^*\gamma^*}(-Q_1^2, -Q_2^2) \mathcal{F}_{p\gamma^*\gamma^*}(-Q_3^2, 0) \Big]$$

We recognize two main objects

1. The TFFs $\mathcal{F}_{p\gamma^*\gamma^*}(q_1^2, q_2^2)$
2. The weight functions $w_i(q_1, q_2, \tau)$

Weight functions are peaked at low spacelike Q^2 so lattice QCD is an appropriate method to compute $a_\mu^{p-\text{pole}}$.

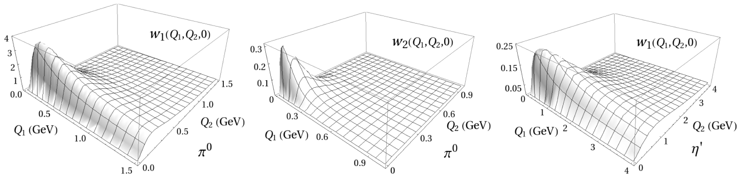

Transition Form Factor from the Lattice

The TFF for a pseudoscalar meson is defined by the matrix elements $M_{\mu\nu}$ (Ji and Jung, 2001) (Gérardin et al., 2016)

$$M_{\mu\nu}(p,q_1) = i\int d^4x\, e^{iq_1\cdot x}\,\langle\Omega|\,T\{J_\mu(x)J_\nu(0)\}\,|P(\vec{p})\rangle = \varepsilon_{\mu\nu\alpha\beta}\,q_1^\alpha q_2^\beta\,\mathscr{F}_{P\gamma^*\gamma^*}(q_1^2,q_2^2)$$

where J_μ is the EM current. The (Euclidean) matrix elements are related to a 3-point correlation function $C_{\mu\nu}$ on lattice

$$C_{\mu\nu}(\tau,t_P) = a^6\sum_{\vec{x},\vec{z}}\langle J_\mu(\vec{z},\tau+t_P)J_\nu(\vec{0},t_P)P^\dagger(\vec{x},0)\rangle e^{i\vec{p}\cdot\vec{x}}e^{-i\vec{q}_1\cdot\vec{z}}$$

where τ is the time-separation between the two EM currents and

1. P is an interpolating operator for the pseudoscalar mesons.
2. In the Euclidean:

$$M^E_{\mu\nu} = \frac{2E_P}{Z_P}\int_{-\infty}^{\infty} d\tau\, e^{\omega_1\tau}\tilde{A}_{\mu\nu}(\tau) \qquad \text{with } \tilde{A}_{\mu\nu}\propto C_{\mu\nu}$$

3. E_P, Z_P energy and overlap of the pseudoscalar that are extracted from two-point correlations functions.
4. $q_1 = (\omega_1,\vec{q}_1)$ and $q_2 = (E_P-\omega_1,\vec{p}-\vec{q}_1)$ with ω_1 a free parameter.
5. For details see (Gérardin et al., 2023).

Reach in (q_1^2, q_2^2) Plane

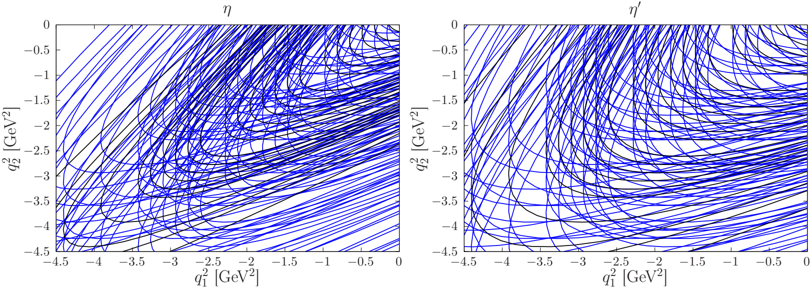

- We have a dense covering of the whole (q_1^2, q_2^2) plane.
- In the rest of the presentation we only display TFF for two kinematics
  (1) $q_1^2 = q_2^2$ (double-virtual)
  (2) $q_1^2 = 0$, $q_2^2 \neq 0$ (single-virtual)

Correlation Function on the Lattice: Wick Contractions

$$C_{\mu\nu}(\tau, t_P) = a^6 \sum_{\vec{x},\vec{z}} \langle J_\mu(\vec{z}, \tau + t_P) J_\nu(\vec{0}, t_P) P^\dagger(\vec{x}, 0) \rangle e^{i\vec{p}\cdot\vec{x}} e^{-i\vec{q}_1\cdot\vec{z}}$$

The correlation function receives contributions from (potentially) four different Wick contractions

1. - For the π^0

$$P_{\pi^0}(x) = \frac{1}{\sqrt{2}} \left(\overline{u}\gamma_5 u(x) - \overline{d}\gamma_5 d(x) \right)$$

! We work in the isospin limit $\Rightarrow$ (2) and (4) do not contribute.

! Diagram (3) is small $\mathcal{O}(1-2\%)$ (Gérardin et al., 2019).

2. - For the η, η'

$$P_{\eta_8}(x) = \frac{1}{\sqrt{6}} \left(\overline{u}\gamma_5 u(x) + \overline{d}\gamma_5 d(x) - 2\overline{s}\gamma_5 s(x) \right)$$

$$P_{\eta_0}(x) = \frac{1}{\sqrt{3}} \left(\overline{u}\gamma_5 u(x) + \overline{d}\gamma_5 d(x) + \overline{s}\gamma_5 s(x) \right)$$

! **All** four diagrams contribute.

! Disconnected diagram (2) is large!

! η_8 and η_0 mix to create physical η, η'.

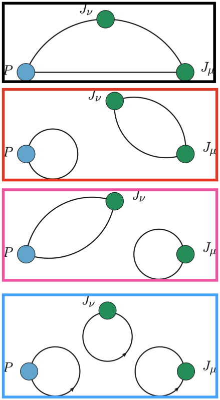

From top to bottom: connected, p.vv, pv.v, p.v.v

Gauge Ensembles

$2+1+1$ dynamical staggered fermions with 4 steps of stout smearing
(subset of ensembles used for the LO HVP calculation (Borsanyi et al., 2021))

- Gauge ensembles at (nearly) physical pion & kaon mass.
- Exploit up to six different lattice spacings ranging between [0.06 - 0.13] fm.
- Consider boxes of $\sim 3, 4$ and 6 fm for finite-size effect studies.
- Ensembles in isosymmetric limit ($\rightarrow$ no mixing between π^0 and $\eta^{(\prime)}$).

Integrand for the Different Wick Contractions (η, η')

Due to staggered oscillations in the integrand, we prefer to display the smeared integrand for clarity. We defined

$$f(\tau)|_{\text{smr}} = \frac{1}{4}f(\tau - a) + \frac{1}{2}f(\tau) + \frac{1}{4}f(\tau + a). \quad (1)$$

In practice, we always integrate the unsmeared integrands!

Left: η

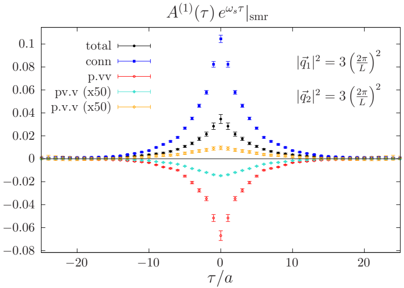

Right: η'

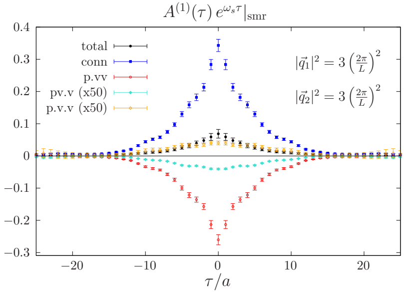

1. We find a signal for all the disconnected diagrams.
2. The connected and p.vv diagrams are the dominant contributions to the signal (but with opposite signs) for both the η and η'.

Fitting the TFF

Continuous description of the TFF can be obtained using the (modified) $z-$**expansion**,

$$P(Q_1^2,Q_2^2)\mathscr{F}_{\pi^0\gamma^*\gamma^*}(-Q_1^2,-Q_2^2) = \sum_{n,m=0}^{N} c_{nm}(a)\left(z_1^n + (-1)^{N+n}\frac{n}{N+1}z_1^{N+1}\right)\times \left(z_2^m + (-1)^{N+m}\frac{m}{N+1}z_2^{N+1}\right),$$

where z_k are conformal variables

$$z_k = \frac{\sqrt{t_c+Q_k^2}-\sqrt{t_c-t_0}}{\sqrt{t_c+Q_k^2}+\sqrt{t_c-t_0}}, \quad k=1,2,$$

- $c_{nm}(a)$ symmetric coefficients
- t_0 free parameter

  - $t_c = 4m_\pi^2$
  - $P(Q_1^2,Q_2^2)$ imposes short distance constraints

The coefficients are expanded as: $c_{nm}(a) = c_{nm}^{(0)}\left(1+\gamma_{nm}a^2+\dots\right)$.

Advantages of z-expansion:

→ Fit is model-independent, only systematic is choice of N.

→ Obtain TFF in whole (Q_1^2,Q_2^2)-plane.

Transition Form Factor π^0 at the physical point

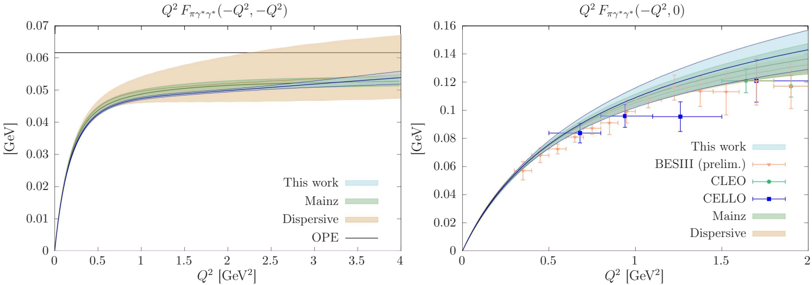

- Good agreement with experimental data.
- Reasonable agreement with previous lattice result (Mainz) and dispersive approach.

Transition Form Factor η at the physical point

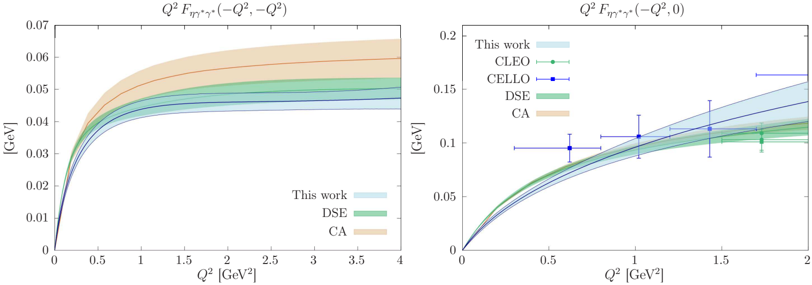

- Good agreement with experimental data but slight tension with lowest CELLO bin.
- Tension below 0.4 GeV^2 with other estimates (DSE and CA)

Transition Form Factor η' at the physical point

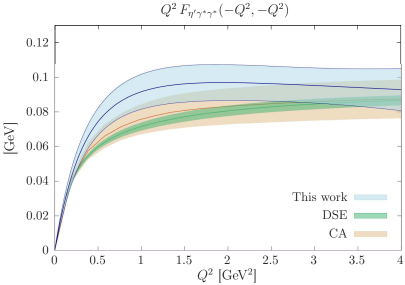

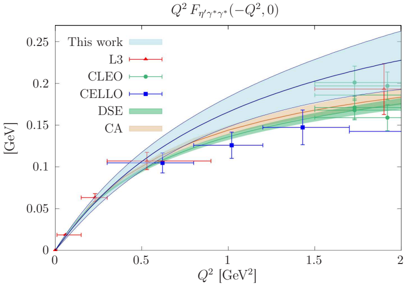

- Reasonable agreement with experimental data.
- Slightly overshoot CELLO data but within 2σ.

Normalization Transition Form Factor

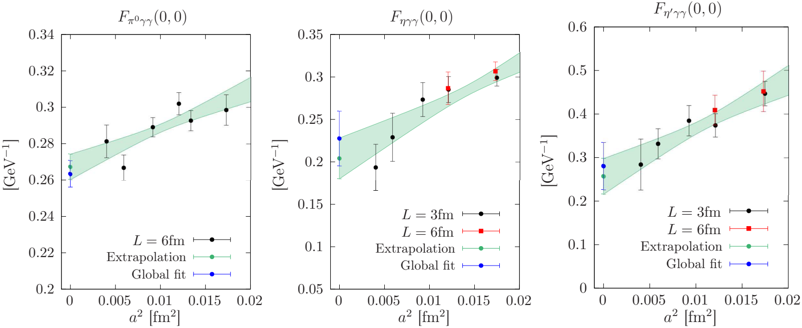

- Good agreement between different large-volume ensembles for the pion TFF.
- Good agreement between large and small-volume ensembles for the η, η' TFF.

Normalization Transition Form Factor

Normalization of TFF related to partial decay widths $\Gamma(p \to \gamma\gamma)$,

$$\Gamma(p \to \gamma\gamma) = \frac{\pi\alpha^2 m_p^3}{4} \mathscr{F}_{p\gamma^*\gamma^*}(0,0).$$

Our results and that of experiment are

	This work	Experiment
$\Gamma(\pi^0 \to \gamma\gamma)$ [eV]	$7.11 \pm 0.44_{\text{stat}} \pm 0.21_{\text{syst}}$	$7.802(52)_{\text{stat}}(105)_{\text{syst}}$
$\Gamma(\eta \to \gamma\gamma)$ [eV]	$338 \pm 94_{\text{stat}} \pm 35_{\text{syst}}$	516 ± 18
$\Gamma(\eta' \to \gamma\gamma)$ [keV]	$3.4 \pm 1.0_{\text{stat}} \pm 0.4_{\text{syst}}$	4.28 ± 0.19

Experimental values from (Larin et al., 2020; PDG, 2020)

Example of Continuum Extrapolation $a_\mu^{p-\text{pole}}$

Reminder

$$a_\mu^{p-pole} = \left(\frac{\alpha_e}{\pi}\right)^3 \int_0^\infty dQ_1 \int_0^\infty dQ_2 \int_{-1}^1 d\tau \left[w_1(Q_1,Q_2,\tau)\mathcal{F}_{p\gamma^*\gamma^*}(-Q_1^2,-Q_3^2)\mathcal{F}_{p\gamma^*\gamma^*}(-Q_2^2,0) + w_2(Q_1,Q_2,\tau)\mathcal{F}_{p\gamma^*\gamma^*}(-Q_1^2,-Q_2^2)\mathcal{F}_{p\gamma^*\gamma^*}(-Q_3^2,0)\right]$$

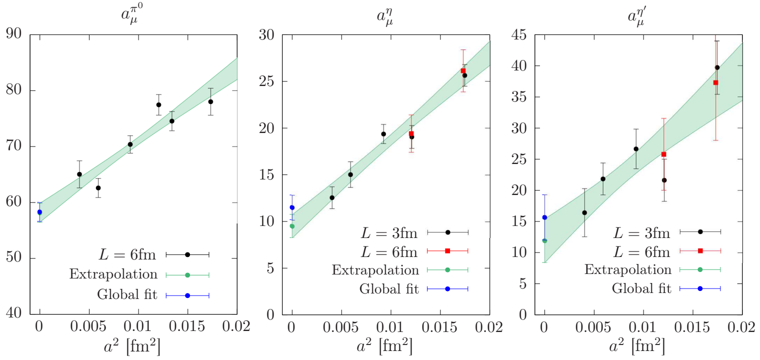

- The extrapolation and global fit procedure agree well within errors for the three mesons.
- We only use large-volume ensembles for the π^0 and they are in good agreement.
- Large- and small-volume ensembles agree well for the $a_\mu^{\eta-\text{pole}}$ and $a_\mu^{\eta'-\text{pole}}$.

Systematics

Different systematic choices in the analysis are varied (for details see (Gérardin et al., 2023))

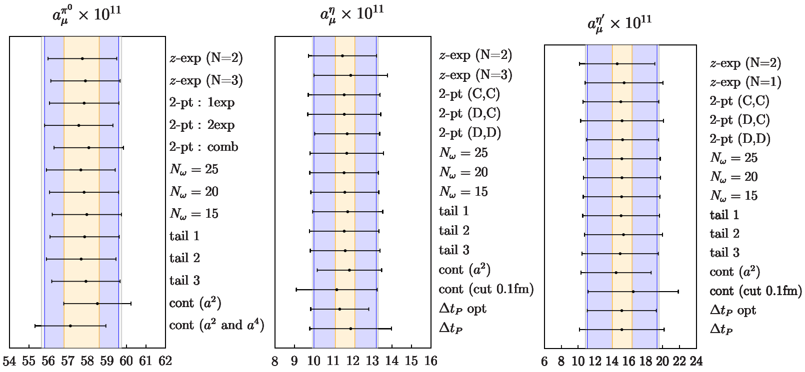

- Points indicate model average over all variations with that specific choice.
- Different bands indicate systematic (yellow), statistical (blue) and total error (grey).
- The systematic error is estimated using assuming flat weight among all variations (since we do not always include all correlations).

Finite Size Effects

Reminder

$$a_\mu^{p-pole} = \left(\frac{\alpha_e}{\pi}\right)^3 \int_0^\infty dQ_1 \int_0^\infty dQ_2 \int_{-1}^1 d\tau \, \big[w_1(Q_1,Q_2,\tau)\mathscr{F}_{p\gamma^*\gamma^*}(-Q_1^2,-Q_3^2)\mathscr{F}_{p\gamma^*\gamma^*}(-Q_2^2,0) + w_2(Q_1,Q_2,\tau)\mathscr{F}_{p\gamma^*\gamma^*}(-Q_1^2,-Q_2^2)\mathscr{F}_{p\gamma^*\gamma^*}(-Q_3^2,0)\big]$$

- $a_\mu^{\eta-\mathrm{pole}}$ and $a_\mu^{\eta'-\mathrm{pole}}$ are computed using mostly $L = 3$ fm volumes.
- Therefore, we compute the $a_\mu^{\pi^0-\mathrm{pole}}$ on $L = 6$ fm and $L = 3$ fm volumes with the weight functions w_1, w_2 of the η, η' and use the difference as a systematic for $a_\mu^{\eta-\mathrm{pole}}, a_\mu^{\eta'-\mathrm{pole}}$.

Pseudoscalar-pole Contributions to a_μ

We find the following values

$$
\begin{aligned}
a_\mu^{\pi^0-\mathrm{pole}} &= (57.8 \pm 1.8_{\mathrm{stat}} \pm 0.9_{\mathrm{syst}}) \times 10^{-11}, \\
a_\mu^{\eta-\mathrm{pole}} &= (11.6 \pm 1.6_{\mathrm{stat}} \pm 0.5_{\mathrm{syst}} \pm 1.1_{\mathrm{FSE}}) \times 10^{-11}, \\
a_\mu^{\eta'-\mathrm{pole}} &= (15.7 \pm 3.9_{\mathrm{stat}} \pm 1.1_{\mathrm{syst}} \pm 1.3_{\mathrm{FSE}}) \times 10^{-11}.
\end{aligned}
$$

$\rightarrow a_\mu^{\eta-\mathrm{pole}}$ and $a_\mu^{\eta'-\mathrm{pole}}$ make up about 1/2 of $a_\mu^{\pi^0-\mathrm{pole}}$.

This leads to

$$
a_\mu^{p-\mathrm{pole}} = (85.1 \pm 4.7_{\mathrm{stat}} \pm 2.3) \times 10^{-11}\,.
$$

This can be compared with WP estimate $a_\mu^{p-\mathrm{pole}} = 93.8^{+4.0}_{-3.6} \times 10^{-11}$ (Aoyama et al., 2020).

Summary

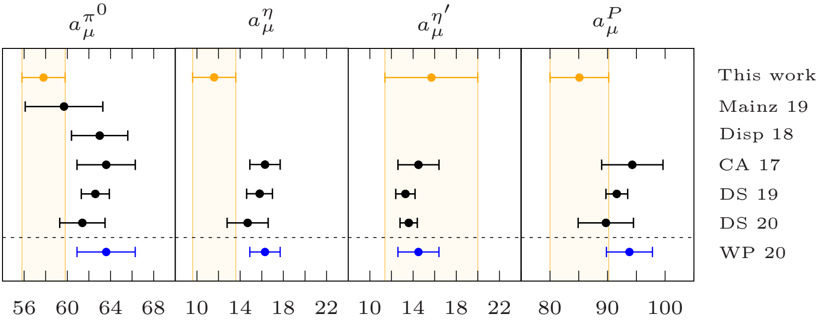

1. Summary:
   - We presented the first ab-initio determination of the TFFs of the π^0, η and η' mesons at the physical point and in the continuum limit.
   - Our main result is

     $$a_\mu^{p-\text{pole}} = (85.1 \pm 5.2) \times 10^{-11}.$$

     This is compatible with the estimate from the WP within 1.4σ.
   - For more details we refer to our pre-print 2305.04570.
2. Outlook:
   - Add larger volumes at finer lattice spacing to constrain the normalization of the TFF or compute the normalization directly.

References

Aoyama, T. et al. (2020). The anomalous magnetic moment of the muon in the Standard Model. *Phys. Rept.*, 887:1–166.

Borsanyi, S. et al. (2021). Leading hadronic contribution to the muon magnetic moment from lattice QCD. *Nature*, 593(7857):51–55.

Burri, S. A. et al. (2022). Pion-pole contribution to HLbL from twisted mass lattice QCD at the physical point. *PoS*, LATTICE2021:519.

Burri, S. A. et al. (2023). Pseudoscalar-pole contributions to the muon $g-2$ at the physical point. *PoS*, LATTICE2022:306.

Gérardin, A., Meyer, H. B., and Nyffeler, A. (2016). Lattice calculation of the pion transition form factor $\pi^0 \to \gamma^* \gamma^*$. *Phys. Rev. D*, 94(7):074507.

Gérardin, A., Meyer, H. B., and Nyffeler, A. (2019). Lattice calculation of the pion transition form factor with $N_f = 2+1$ Wilson quarks. *Phys. Rev. D*, 100(3):034520.

Gérardin, A., Verplanke, W. E. A., Wang, G., Fodor, Z., Guenther, J. N., Lellouch, L., Szabo, K. K., and Varnhorst, L. (2023). Lattice calculation of the π^0, η and η' transition form factors and the hadronic light-by-light contribution to the muon $g-2$.

References

Hoferichter, M., Hoid, B.-L., Kubis, B., Leupold, S., and Schneider, S. P. (2018). Dispersion relation for hadronic light-by-light scattering: pion pole. *Journal of High Energy Physics*, 2018(10).

Ji, X. and Jung, C. (2001). Studying hadronic structure of the photon in lattice QCD. *Physical Review Letters*, 86(2):208–211.

Knecht, M. and Nyffeler, A. (2002). Hadronic light-by-light corrections to the muon $g-2$: The pion-pole contribution. *Physical Review D*, 65(7).

Larin, I. et al. (2020). Precision measurement of the neutral pion lifetime. *Science*, 368(6490):506–509.

PDG (2020). Review of Particle Physics. *PTEP*, 2020(8):083C01.

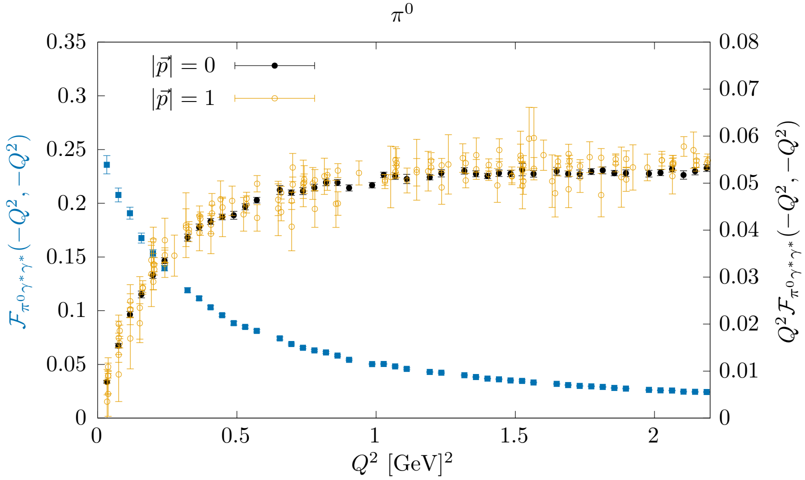

π^0
$|\vec{p}| = 0$
$|\vec{p}| = 1$
$\mathcal{F}_{\pi^0\gamma^*\gamma^*}(-Q^2, -Q^2)$
$Q^2\mathcal{F}_{\pi^0\gamma^*\gamma^*}(-Q^2, -Q^2)$
Q^2 [GeV]^2
0
0.05
0.1
0.15
0.2
0.25
0.3
0.35
0.01
0.02
0.03
0.04
0.05
0.06
0.07
0.08
0.5
1
1.5
2